ELSEVIER

International Journal of Adhesion & Adhesives 27 (2007) 469–479

International Journal of Adhesion & Adhesives

www.elsevier.com/locate/ijadhadh

Properties of thermoplastic polyurethane adhesives containing nanosilicas with different specific surface area and silanol content

José Vega-Baudrit[a], María Sibaja-Ballestero[a], Patricia Vázquez[b], Rosa Torregrosa-Maciá[c], José Miguel Martín-Martínez[c,*]

[a]*Polymer Laboratory—POLIUNA, Universidad Nacional, 86-3000 Heredia, Costa Rica*
[b]*Research and Development Centre for Applied Sciences (CINDECA), CONICET-UNLP, 47 n 257, B1900AJK La Plata, Buenos Aires, Argentina*
[c]*Adhesion and Adhesives Laboratory, University of Alicante, 03080 Alicante, Spain*

Accepted 14 August 2006
Available online 26 September 2006

Abstract

Thermoplastic polyurethane (TPU) adhesives containing nanosilicas with different specific surface area and silanol group content were prepared and characterized by FTIR spectroscopy, differential scanning calorimetry (DSC), thermogravimetry (TGA), X-ray diffraction, plate-plate rheology, dynamical–mechanical–thermal analysis (DMTA), transmission electron microscopy (TEM), and strain–stress test. Adhesive strength was obtained from *T*-peel tests of PVC/polyurethane adhesive joints.

Formation of agglomerates of nanosilica particles within the polyurethane matrix were favoured by increasing the silanol content likely due to stronger hydrogen bond interactions between the silanol groups on the nanosilica over those between the polyurethane and the nanosilica. As a consequence, inter-urethane bonds formation rather than ester-urethane bonds were favoured, leaving the soft segment chains more free to interact between them. Thus, addition of nanosilica favoured the phase segregation in the thermoplastic polyurethane. The increase in specific surface area and silanol content in the nanosilica, generally enhanced the degree of phase separation in the polyurethane, being less marked for nanosilicas with more than 200 m^2/g and 0.60 mmol $SiOH/g_{silica}$. On the other hand, the addition of the nanosilica improved the tensile strength and elongation at break, and the viscoelastic properties of the polyurethane. The immediate adhesive strength of PVC/polyurethane adhesive joints increased in the filled adhesives and it was determined by the rheological properties of the polyurethane–nanosilica mixtures. By increasing the time after joint formation, the crystallization of the polyurethane was produced giving higher adhesive strength and although a cohesive failure in the PVC was always obtained, a slight though progressive increase in joint strength was found with the passage of time with the ordering of the three systems (PU-0.45, PU-0.60 and PU-0.90) remaining unchanged with the PU-0.60 system the stronger and the PU-0.90 system the weaker. This is in agreement with the trends in the viscoelastic and mechanical properties of the filled adhesives.

Keywords: Polyurethane; Infrared spectra; Rheology; Mechanical properties of adhesives

1. Introduction

Thermoplastic polyurethanes (TPUs) are multi-phase segmented polymers that exhibit a two-phase microstructure (i.e. phase separation), which arises from the incompatibility between the soft and the hard segments. The hard rigid segment segregates into a glassy or semicrystalline domain, and the polyol soft segments form amorphous or rubbery matrices in which the hard segments are dispersed [1]. TPUs are commonly used as adhesives to join different materials in the footwear, automotive and general use adhesives industries.

Fumed silicas (nanosilicas) are fillers commonly added to improve the thermal, rheological and mechanical properties of TPU adhesives [2–7]. This improvement in properties has been previously ascribed to the creation of hydrogen bonds between the hydroxyl groups on the nanosilica surface and the soft segments of the polyurethane, favouring the degree of phase separation [8–11].

*Corresponding author. Tel.: +34 96 5903977; fax: +34 96 5903454.
E-mail address: jm.martin@ua.es (J. Miguel Martín-Martínez).

0143-7496/$ - see front matter © 2006 Elsevier Ltd. All rights reserved.
doi:10.1016/j.ijadhadh.2006.08.001

Previous experimental evidence [12] has corroborated the formation of hydrogen bonds between the nanosilica and the polyurethane.

To analyze in depth the creation of hydrogen bonds between the nanosilica and the polyurethane and its incidence in the structure and properties of polyurethane adhesives, three nanosilicas with different specific surface area and silanol contents were added to a thermoplastic polyurethane adhesive. Specific surface area is inversely related to the primary particle size of nanosilica, and the greater the specific surface area the greater the silanol content. If hydrogen bond formation is responsible for improving the properties of nanosilica–polyurethane mixtures, it can be expected that the greater the silanol content in the nanosilica, the more noticeable the extent of phase separation in the polyurethane should be; therefore, 2 wt% of different nanosilicas was added to a TPU and the mixtures obtained were characterized by FTIR spectroscopy, DSC, X-ray diffraction, plate–plate rheometry, DMTA, TEM, stress–strain test and *T*-peel tests.

2. Experimental

2.1. Materials

Three different nanosilicas manufactured by Wacker-Chemie (Burghausen, Germany) were used. According to the manufacturer, the nominal primary particle size in all nanosilicas was 7 nm. Table 1 shows the nomenclature of the nanosilicas and their nominal specific surface areas which, according to Wacker-Chemie, ranged between 150 and 300 m^2/g. As a direct correlation between particle size and specific surface area should exist, the nanosilicas must show different degree of agglomeration (see below).

The thermoplastic polyurethane (TPU) was prepared using the prepolymer method. The prepolymer was obtained by reacting polyadipate of 1,4-butanediol ($M_w = 2440$ Da) with 4,4-diphenyl methane diisocyanate—MDI; a isocyanate/macroglycol equivalent ratio of 1.05 was used. 1,4-butanediol was used as chain extender. High purity solid MDI was supplied by Aldrich (Cat. 25.643-9), and it is a mixture of 98 wt% of the 4,4′-isomer and 2 wt% of the 2,4′-isomer. The NCO content of the prepolymer was determined by titration with dibutylamine (UNE-EN 1242 standard). The polyadipate of 1,4-butanediol (Hoopol F-530) was supplied by Hooker S.A. (Barcelona, Spain) and was heated for 4 h at 70 °C under reduced pressure (5 Torr) to remove the residual water. The 1,4-butanediol was supplied by Aldrich (Cat. B8,480-7) and was dried using 4 Å molecular sieves.

To avoid crosslinking reactions during polyurethane synthesis, the reaction temperature was kept below 65 °C under a stirring speed of 80 rpm. The synthesis of the polyurethane was carried out in dry nitrogen atmosphere to avoid the presence of water in the reactor. The prepolymers containing unreacted isocyanate ends were completely reacted with the necessary stoichiometric amount of 1,4-butanediol. The reaction time was 2 h. The TPUs were annealed in an oven at 80 °C for 12 h.

TPU adhesive solutions were prepared by mixing 20 wt% solid polyurethane and 2 wt% nanosilica with 2-butanone in a Dispermix DL-A laboratory mixer, provided with a Cowles mechanical stirrer (diameter = 50 mm) and a water jacket to maintain the temperature at 25 °C during the preparation of the adhesives. Adhesive preparation was carried out in two consecutive stages: (i) 13.6 g nanosilica was mixed for 15 min at 2500 rpm with 217 g butanone. (ii) 136 g TPU and 433.6 g butanone were added to the previous solution, stirring the mixture for 2 h at 2000 rpm. TPU adhesive solutions were kept in a hermetic container until use. A TPU adhesive solution without silica was also prepared as control. Most of the properties of the polyurethanes were measured using solid films, which were prepared by placing about 100 cm^3 of adhesive solution in a Teflon mould and allowing a slow evaporation of the solvent at room temperature for 2 days. The polyurethane films obtained were about 0.7–0.9 mm thick.

The nomenclature of the polyurethane–nanosilica mixtures was PU0 (TPU without silica), and PU-0.45, PU-0.60 and PU-0.90, for the TPUs containing nanosilicas with silanol content of 0.45 mmol $SiOH/g_{silica}$ (HDK V15), 0.60 mmol $SiOH/g_{silica}$ (HDK N20) and 0.90 mmol $SiOH/g_{silica}$ (HDK T30), respectively.

2.2. Experimental techniques

2.2.1. FTIR spectroscopy

A Bruker IFS 66 FTIR spectrometer (located at the Institut Fertgungstechnik Materialforschung—IFAM, Germany) provided with a photoacoustic cell was used to characterize the chemistry of the nanosilicas. The IR spectra of the polyurethane films were obtained in the

Table 1
Parameters obtained by applying the BET method to the N_2/77 K adsorption isotherms of nanosilicas with different specific surface area

Nanosilica	Specific surface area (m^2/g)		C_{BET} parameter	Silanol content (mmol $SiOH/g_{silica}$)[a]
	Nominal[a]	Experimental		
HDK V15	150 ± 20	129	96	0.45
HDK N20	200 ± 30	179	114	0.60
HDK T30	300 ± 30	215	142	0.90

[a]Data provided by Wacker-Chemie.

transmission mode using a Bruker Tensor 27 spectrophotometer. Under the experimental conditions used, the signal/noise ratio of the equipment was 0.04% transmittance (at 2000 cm^{-1}). The resolution was 4 cm^{-1} and 80 scans were recorded and averaged.

2.2.2. N_2/77 K adsorption isotherms

The specific surface area of the nanosilicas was obtained from N_2/77 K adsorption isotherms measured in a Quantachrome adsorption system. Prior to adsorption measurements, the nanosilicas were out-gassed at 100 °C for 8 h under a residual pressure of 10^{-6} Torr.

2.2.3. Differential scanning calorimetry (DSC)

DSC experiments were carried out in a TA instrument DSC Q100 V6.2. Aluminium pans containing 12–15 mg of sample were heated from −80 °C to 80 °C under nitrogen atmosphere. The heating rate was 10 °C/min. The first heating run was carried out to remove the thermal history of the samples. From the second heating run, the glass transition temperature (T_g), the melting temperature (T_m), the crystallization temperature (T_c), the melting enthalpy (ΔH_m), and the crystallization enthalpy (ΔH_c) of the TPUs were obtained. The crystallization rate was estimated by melting the polyurethane film at 100 °C, followed by a sudden decrease to 25 °C and the evolution of heat with time under isothermal conditions was monitored for 30 min at 25 °C until a crystallization peak appeared.

2.2.4. Thermogravimetry (TGA)

TGA studies were carried out in a Mettler TGSDTA thermobalance, model 851e/1600/LF, in nitrogen flow at a rate of 100 ml/min. Samples (4–5 mg) were heated under nitrogen from room temperature up to 800 °C by using a heating rate of 10 °C/min.

2.2.5. Wide angle X-ray diffraction (WAXD)

The polyurethane crystallinity was determined using Seifert model JSO-DEBYEFLEX 2002 equipment. This equipment was provided with a copper cathode and a nickel filter, and the monochromatic radiation of copper (K_α) was used as the X-ray source ($\lambda = 1.54$ Å). A range of diffraction angles (2θ) from 5° to 90° were used in the experiments.

2.2.6. Plate–plate rheometry

The rheological properties of the polyurethane films were determined in a shear stress-controlled Bohlin CS50 rheometer, using parallel plates (upper plate diameter = 20 mm); the gap selected was 0.4 mm.Oscillatory experiments were performed to determine the rheological properties (mainly the storage, G', and loss, G'', moduli) of the polyurethane films. Experiments were performed by melting the polyurethane film at 200 °C and cooling down to 30 °C at a cooling rate of 5 °C/min; the target strain was 0.005 and the frequency was set to 1 Hz. All the experimental results were obtained in the region of linear viscoelasticity.

2.2.7. Dynamic mechanical thermal analysis (DMTA)

The viscoelastic properties of the polyurethanes were measured in a Rheometric Scientific DMTA Mk III instrument using the two-point bending mode (single cantilever). The experiments were carried out by heating the sample from −80 °C to 100 °C, using a heating rate of 5 °C/min, a frequency of 1 Hz and a strain of 64 μm peak–peak.

2.2.8. Transmission electron microscopy (TEM)

A JEOL JEM-2010 instrument was used to analyze the morphology of the nanosilicas; an acceleration voltage of 100 kV was used. The nanosilicas were placed directly into the grid specially design for TEM analysis.

2.2.9. Stress–strain measurements

The tensile strength and elongation at break of the polyurethane films were obtained in an Instron 1011 using dog-bone test pieces of 0.8 mm thick and 4 mm width (in the centre of the test sample) and following the test procedure given in the ISO 37–77 standard; a cross-head rate of 100 mm min^{-1} was used.

2.2.10. T-peel strength measurements

Adhesive strength was obtained from *T*-peel tests of solvent-wiped plasticized PVC/polyurethane adhesive joints. Table 2 shows the composition of the plasticized PVC used to prepare the adhesive joints. The PVC test samples used had dimensions of 30 mm × 150 mm × 5 mm. Before applying the adhesive, the smooth PVC surface was wiped by rubbing the surface with a cotton cloth soaked in butanone and allowing the solvent to evaporate for 30 min. After the solvent wiping of the PVC, 1.5 ml of adhesive solution was applied by brushing to each strip to be joined, and left to dry for 1 h in air. After evaporation, a uniform without bubbles solid polyurethane film of about 100 μm thick (measured from SEM micrographs of sections) was formed which was rapidly heated to 80 °C by infrared radiation (reactivation process). The strips were immediately placed in contact at 80 °C and a pressure of 0.8 MPa was applied for 10 s to achieve a suitable joint. The *T*-peel strength was measured at room temperature in an Instron

Table 2
Composition of the plasticized poly(vinyl chloride) (PVC) used in the *T*-peel tests

Ingredient	Percentage (by weight)
Poly(vinyl chloride)	57.1
Di-octyl phthalate	36.5
Epoxidized soy oil	1.9
Calcium carbonate	2.3
Stabilizer	1.7
Titanium dioxide	0.5

1011 instrument at a crosshead speed of 100 mm/min. The values obtained were the average of five replicates (standard deviation was less than 5%). After joint formation, the soft segments in the polyurethane tend to organize themselves producing crystallization. Because of this, the evolution of the *T*-peel strength was monitored at different times after joint formation (0.5–120 h).

3. Results and discussion

3.1. Characterization of the nanosilicas

The IR spectra of the three nanosilicas (Fig. 1) are relatively similar and show the broad stretching band of the Si–OH group at 3731 cm^{-1}, the bending band of Si–O at 1225 cm^{-1}, and the two stretching bands of Si–O–Si at 1110 and 810 cm^{-1}. Furthermore, broad bands at 3451 and 1710–1625 cm^{-1} appear due to the associated water molecules on the nanosilica surface.

The differences in silanol content on the nanosilicas were calculated by plotting the ratio of the intensities of the IR bands at 3731 cm^{-1} (characteristic of the silanol groups) and at 1110 cm^{-1} (Si–O–Si band, whose intensity does not vary in the three nanosilicas). According to Fig. 2, the nanosilica with the highest silanol content (0.90 mmol $SiOH/g_{silica}$) shows the highest intensities ratio and that with a specific surface area of 200 m^2/g, the lowest one. This trend is not in agreement with the expected increase in hydrogen bonding between silanol groups on the nanosilica that should be favoured by increasing the silanol content. Likely, the presence of water should reduce the intensity of the band at 3731 cm^{-1} in the IR spectrum of HDK N20.

The silanol content can be related to the hydrophilicity of the nanosilicas and this can be estimated from wettability experiments by using polar liquids with different ability of hydrogen bond formation. Water, ethanol and water–ethanol (1:1 in volume) were used as tests liquids, as hydrogen bond formation is highly favoured in water and almost absent in ethanol. The lowest the volume of test liquid needed to wet the nanosilica, the lowest its hydrophilicity. Table 3 shows that an increase in the silanol content on the nanosilica increases the volume of the test liquids and thus the hydrophilicity increases, more markedly in the nanosilica having 0.60 mmol $SiOH/g_{silica}$. Whereas, the nanosilica with the lowest silanol content needs a similar volume to be wetted by the three test liquids, the nanosilicas with 0.60 and 0.90 mmol $SiOH/g_{silica}$ show an increase in the order water <ethanol–water <ethanol. Therefore, the HDK T30 nanosilica shows the highest wettability and the greatest hydrophilicity, and the HDK V15 nanosilica has the lowest wettability and hydrophilicity.

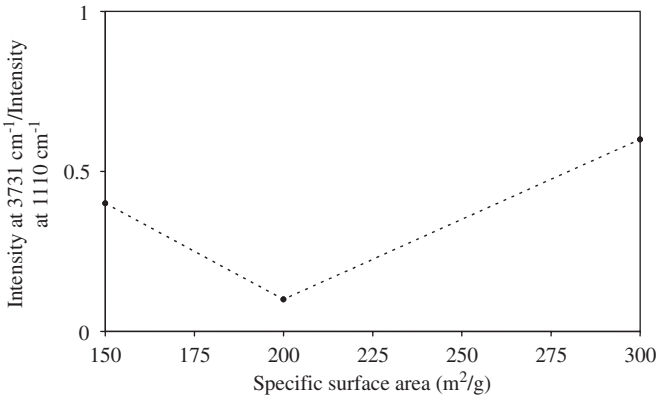

Fig. 2. Variation of the ratio of the intensities of the bands at 3731 and 1110 cm^{-1} in the IR spectra of Fig. 1, as a function of the specific surface area of the nanosilicas.

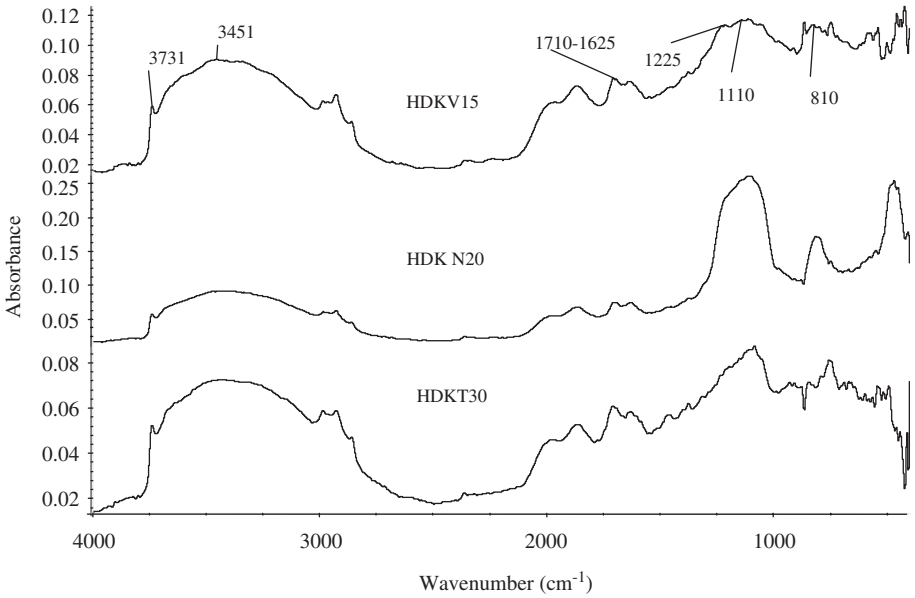

Fig. 1. IR spectra of the nanosilicas.

Table 3
Wettability of nanosilicas obtained with different test liquids

Nanosilica	Silanol content (mmol SiOH/g_{silica})	Test liquids		
		H_2O (ml/g_{silica})	H_2O + EtOH (ml/g_{silica})	EtOH (ml/g_{silica})
HDK V15	0.45	1.1	1.1	1.8
HDK N20	0.60	9.3	11.2	15.8
HDK T30	0.90	12.6	12.9	15.4

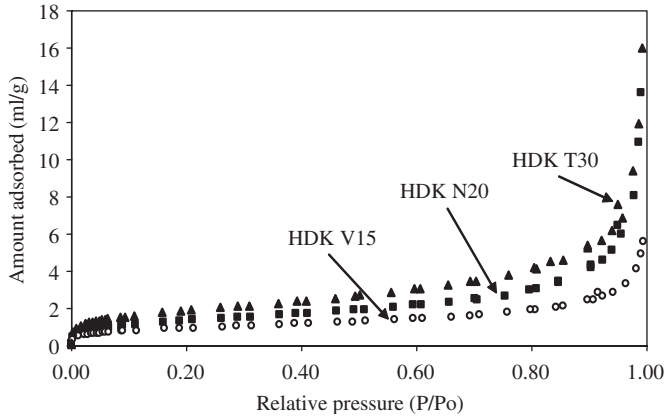

Fig. 3. N_2/77 K adsorption isotherms of the nanosilicas.

Fig. 3 shows the N_2/77 K adsorption isotherms of the nanosilicas. The isotherms correspond to the type II according to the Brunauer–Deming–Deming–Teller classification [13], which is typical of nonporous materials. The monolayer region is well defined and capillary condensation is noticed by a sudden increase in amount adsorbed at high relative pressure. The amount adsorbed of nitrogen increases in the order HDK V15 > HDK N20 > HDK T30. For HDK V15, the capillary condensation starts at a relative pressure of 0.90, whereas for HDK N20 it begins at a relative pressure of 0.85 and for HDK T30 at 0.70. A noticeable increase in amount adsorbed of nitrogen due to capillary condensation is produced due to the smaller particle size of the nanosilicas. The application of the BET equation [13] in the region of relative pressure between 0.05 and 0.30 allows the calculation of the monolayer adsorption capacity in ml/g (V_m) of the nanosilicas

$$\frac{(P/P_o)}{[V(1-P/P_o)]} = \frac{1}{(V_m C)} + \frac{(C-1)(P/P_o)}{(V_m C)}, \quad (1)$$

where V is the amount adsorbed of N_2 in ml/g, P/P_o is the relative pressure, and C is a parameter related to the adsorptive–nanosilica interactions.

The specific surface area (S_{BET}) was obtained from the V_m values by applying

$$S_{BET} = \frac{a_m V_m N_A}{v_M}, \quad (2)$$

where a_m is the cross-section of the N_2 molecule (16.2×10^{-20} m^2), N_A is the Avogadro number, and v_M is the N_2 molar volume (22414 cm^3/mol).

The specific surface area and the C_{BET} parameter of the nanosilicas are given in Table 1. The specific surface area decreases in the order HDK T30 > HDK N20 > HDK V15, the experimental values being lower than the nominal ones provided by Wacker likely due to the tendency of nanosilicas to agglomerate because of hydrogen bonding between silanol groups. The degree of agglomeration is more noticeable by increasing the specific surface area of the nanosilica (Fig. 4). On the other hand, the C_{BET} parameter is an indication of the nitrogen–nanosilica

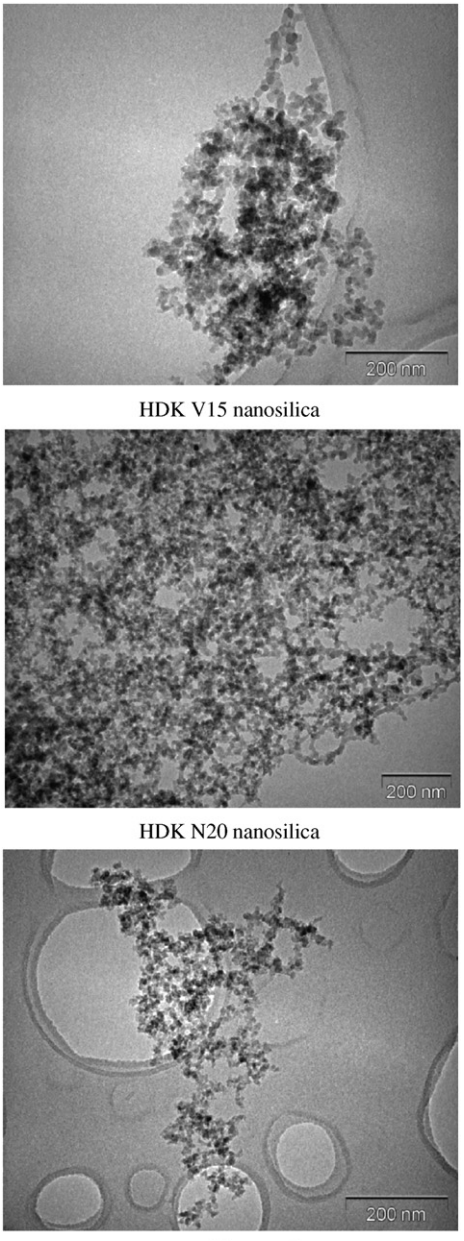

Fig. 4. TEM micrographs of the nanosilicas.

surface interactions and it increases when the specific surface area of the nanosilica increases.

Fig. 4 shows the TEM micrographs of the nanosilicas. All nanosilicas have a primary particle size in the nanometer scale and they tend to agglomerate. The agglomerate size increases by increasing the silanol content on the HDK N20 and HDK T30 nanosilicas. However, the size of the aggregates in the nanosilica with the lower silanol content (HDK V15) is the most pronounced. This must be due to the experimental conditions used during the preparation of HDK V15 for carrying out the TEM measurements.

3.2. Characterization of the nanosilica–polyurethane films

Fig. 5 shows the IR spectra of the nanosilica–polyurethane films. All IR spectra show the bands of the polyurethanes at 3440 (free N–H stretching), 3354 (hydrogen-bonded N–H), 1727 (C═O of urethane), 1595 (N–H bending) and 1530 cm^{-1} (C–N). The bands due to the C–O–C of the polyester at 1174 and 1455 cm^{-1} also appear. Because the band due to the isocyanate at 2250 cm^{-1} is not present, the polyurethane is fully reacted. The nanosilica–polyurethane mixtures also show the bands due to silica at 1069–1077 (Si–O–C and Si–O–Si) and 820 cm^{-1} (Si–OH and Si–O–Si). There are no noticeable differences between the IR spectra of the polyurethane–nanosilica mixtures with different silanol contents likely due to the small amount added to the polyurethane. Only for the nanosilica–polyurethane mixture containing the nanosilica with 0.60 mmol $SiOH/g_{silica}$, a more intense band at 1077 cm^{-1} can be noticed.

The IR stretching bands at 3440 and 3354 cm^{-1} correspond to free (NH_{free}) and hydrogen-bonded (NH_{bonded}) N–H in the polyurethane, respectively. From the relative intensity of these bands it is possible to calculate the degree of phase separation (DPS) in the polyurethane–nanosilica mixtures by using

$$DPS = \frac{NH_{bonded}}{NH_{bonded} + NH_{free}}. \quad (3)$$

Whereas the addition of HDK V15 nanosilica does not affect the degree of phase separation of the polyurethane, the increase in the silanol content of the nanosilica produces an increase which is more marked for the nanosilica containing 0.60 mmol $SiOH/g_{silica}$ (Fig. 6). It seems that the interactions between the polyurethane and the silanol groups on the nanosilica are produced. Two

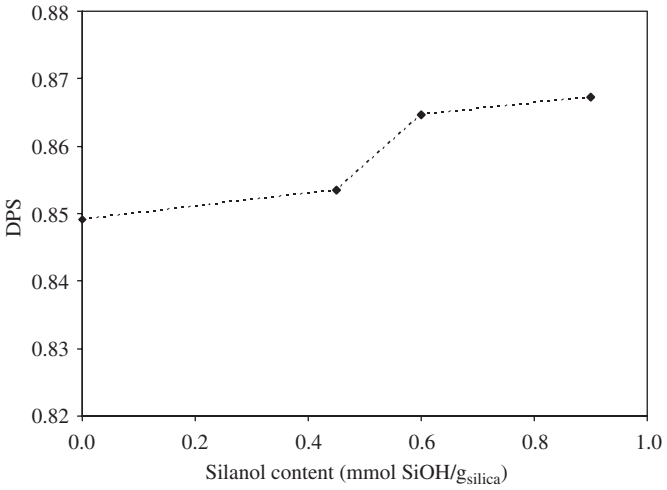

Fig. 6. Degree of phase separation (DPS) in the nanosilica–polyurethane mixtures as a function of the silanol content on the nanosilicas.

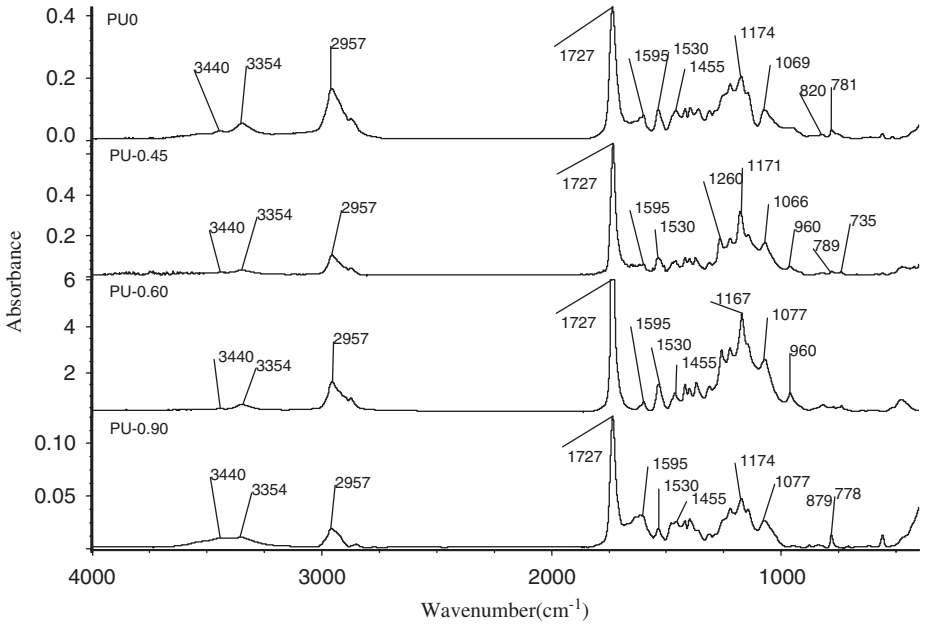

Fig. 5. IR spectra of the nanosilica–polyurethane mixtures.

kinds of hydrogen bond interactions can be distinguished in polyurethanes, inter-urethane and ester-urethane, the former being stronger. When potential hydrogen-bond forming species, such as silanol groups on the nanosilica, are added the association–dissociation equilibrium of the hydrogen bond in the polyurethane can be altered as inter-urethane hydrogen bonds should be favoured, facilitating the mobility of the soft segments. Thus, the soft segments in the polyurethane are reorganized creating more soft domains and producing a greater degree of phase separation. The increase in the silanol content on the nanosilica increases the degree of phase separation in the polyurethane.

The degree of phase separation affects the thermal properties and crystallinity of the polyurethanes. The thermal properties of the nanosilica–polyurethane mixtures were characterized by DSC and TGA. The crystallinity of the nanosilica–polyurethane mixtures was obtained by X-ray diffraction.

The DSC thermograms of the nanosilica–polyurethane mixtures are given in Fig. 7. They show one T_g value located at low temperature due to the soft segments followed by the cold crystallization of these soft segments (i.e. an exothermal peak), and the melting of the soft segments (located at higher temperature). The glass-transition temperature values of the nanosilica–polyurethane mixtures are given in Table 4, and they are similar between them irrespective of the silanol content of the nanosilica. However, the addition of the nanosilica affects the crystallization of the polyurethane. The cold crystallization of all polyurethanes is located near −14 °C but the enthalpy of crystallization decreases by adding nanosilica, which is in agreement with the lower degree of phase segregation in the polyurethane without nanosilica (PU0). Similarly, the melting of the soft segments in all polyurethanes is produced at about 45 °C but the melting enthalpy decreases by adding nanosilica and more markedly by increasing its silanol content. This trend is in agreement with the increase in the degree of phase separation of Fig. 6.

The thermal degradation of the nanosilica–polyurethane mixtures was analyzed by TGA experiments (Fig. 8). The decomposition of the mixtures is produced at about 400 °C in a short range of temperature. Whereas the decomposition of the polyurethane starts at 380 °C, for the nanosilica–polyurethane mixtures the decomposition starts at higher temperature (384 °C for PU-0.45, 390 °C for PU-0.60, and 386 °C for PU-0.90). Therefore, the addition of

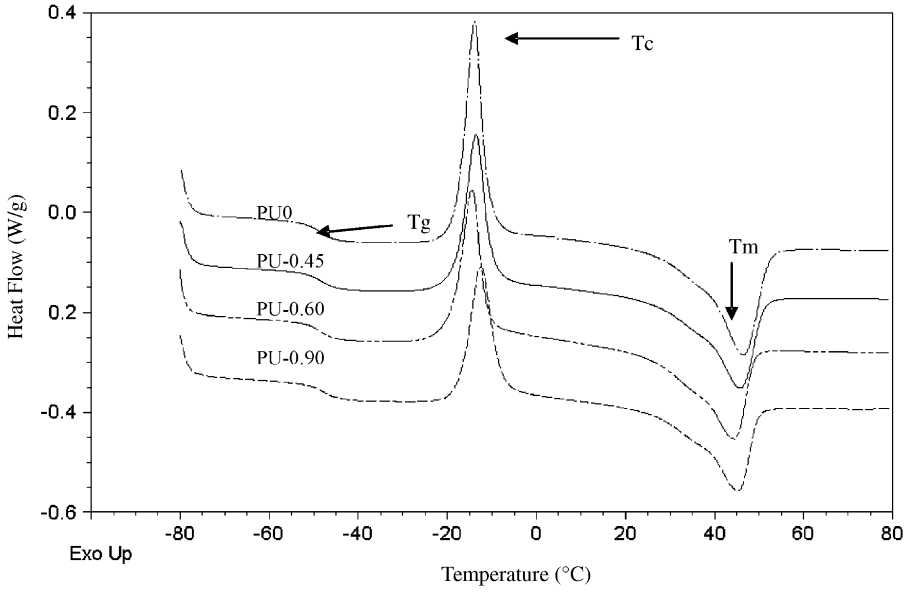

Fig. 7. DSC thermograms of the nanosilica–polyurethane mixtures. Second heating run.

Table 4
Some parameters obtained from the DSC curves (Fig. 7) of the nanosilica–polyurethane mixtures

Nanosilica–polyurethane	T_g (°C)	Crystallization temperature (°C)	Crystallization enthalpy (J/g)	Melting temperature (°C)	Melting enthalpy (J/g)
PU0	−49	−14	−29.3	47	30.8
PU-0.45	−48	−14	−22.2	46	26.5
PU-0.60	−49	−14	−22.1	44	25.8
PU-0.90	−48	−12	−21.2	45	23.3

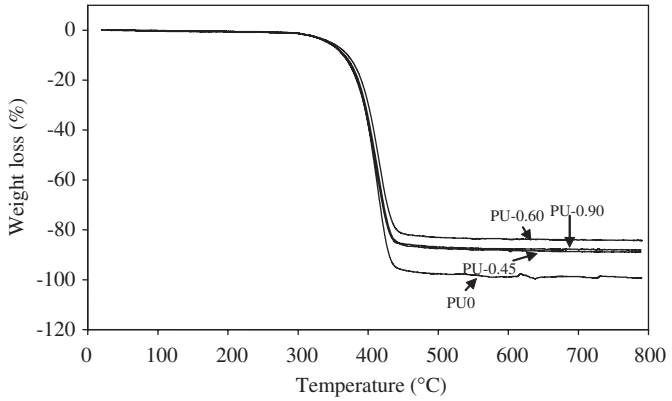

Fig. 8. TGA thermograms of the nanosilica–polyurethane mixtures.

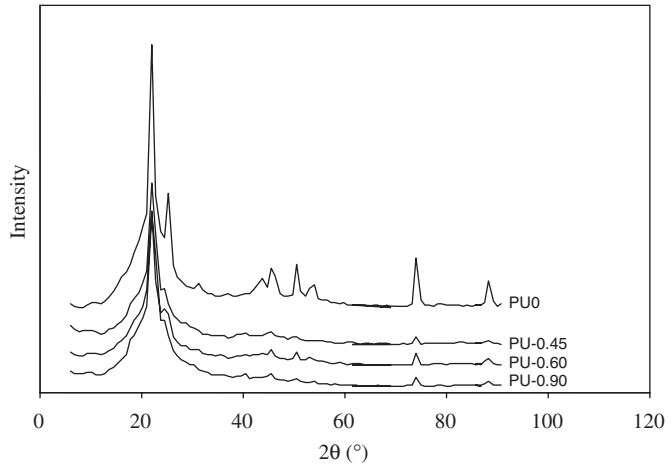

Fig. 9. X-ray diffractograms of the nanosilica–polyurethane mixtures.

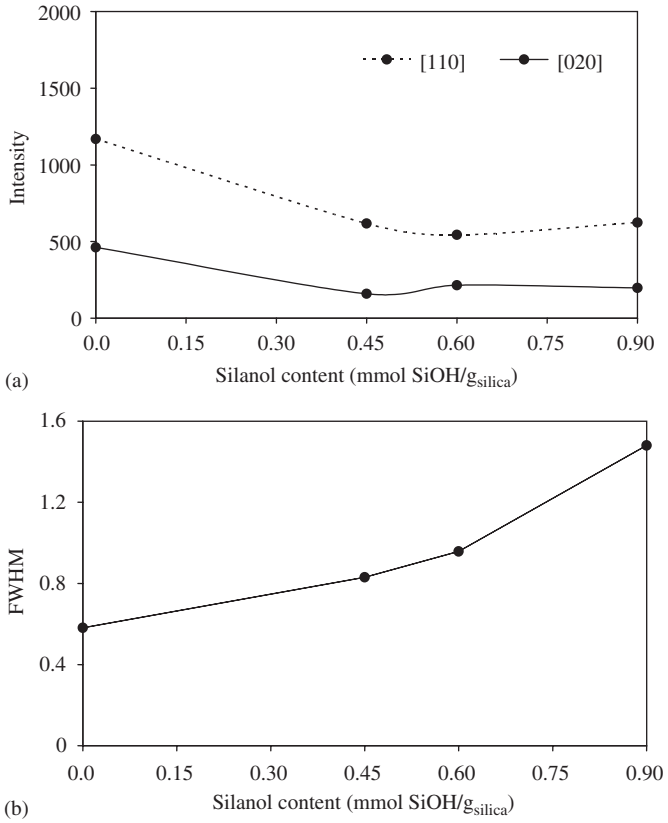

Fig. 10. (a) Variation of the intensities of the diffraction signals of the polyurethanes at 2θ values of 20° and 25° as a function of the silanol content on the nanosilicas. (b) Variation of the full-width at half-maximum (FWHM) of the polyurethanes at $2\theta = 21.5°$ as a function of the silanol content on the nanosilicas.

nanosilica slightly increases the thermal stability of the polyurethane. On the other hand, some ashes (i.e. residual weight at temperatures higher than the decomposition temperature) for nanosilica–polyurethane mixtures can be noticed.

The X-ray diffractograms of the nanosilica–polyurethane mixtures (Fig. 9) show several diffraction peaks, being the main ones located at 2θ values of 20°, 22° and 25°, which correspond to the (1 1 0), (1 0 1) and (0 2 0) planes of the monoclinic cell of polyadipate of 1,4-butanediol, respectively. The addition of the nanosilicas produces a decrease in the crystallinity of the polyurethane (Fig. 10a), i.e. a decrease in the intensity of the diffraction signals at (1 1 0) and (0 2 0) is produced; the magnitude of this decrease is not depending on the specific surface area and silanol content of the nanosilica. Therefore, the crystallinity of the polyurethane decreases because of the increase in the degree of phase separation caused by the nanosilica. The width at half of the diffraction peak is inversely proportionate to the crystallite size. The full-width at half-maximum (FWHM) value of the polyurethane at 2θ of 21.5° (Fig. 10b) increases by adding nanosilica and in a greater extent by increasing the silanol content. Therefore, PU0 has the largest crystallite size and PU-0.90 the smallest.

The addition of nanosilicas with different specific surface areas and silanol contents also affects the rheological and viscoelastic properties of the polyurethanes. The characterization of the nanosilica–polyurethane mixtures by using plate–plate rheometry is given in Figs. 11a and b. The elastic or storage modulus (G') of the polyurethanes decreases by increasing the temperature (Fig. 11a). The addition of nanosilica produces an increase in the storage modulus of the polyurethane and there is a less marked decrease of the storage modulus by increasing the temperature, as compared to PU0. The higher the silanol content on the nanosilica, the less marked decrease of the storage modulus with the temperature. These evidences confirm the creation of hydrogen bonds between the polyurethane and the silanol groups on the silica, in a greater extent by increasing the silanol content on the nanosilica. By plotting together both the storage (G') and the loss (G'') moduli as a function of the temperature (Fig. 11b) the existence of a cross-over at 85 °C for the polyurethane without nanosilica can be noticed, i.e. at temperatures below 85 °C the polyurethane behaviour is mainly elastic and at higher temperatures its viscous behaviour dominates. This cross-over disappears by adding

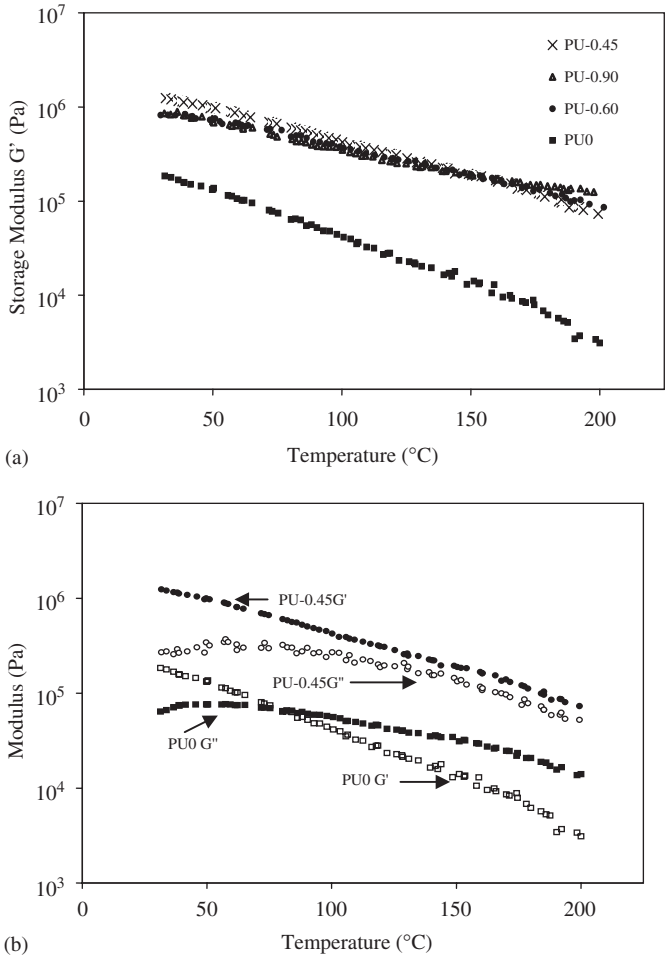

Fig. 11. (a) Variation of the storage module (G') of the nanosilica–polyurethane mixtures as a function of the temperature. (b) Variation of the storage (G') and loss (G'') moduli of PU0 and PU-0.45 as a function of the temperature. Plate–plate rheometry experiments.

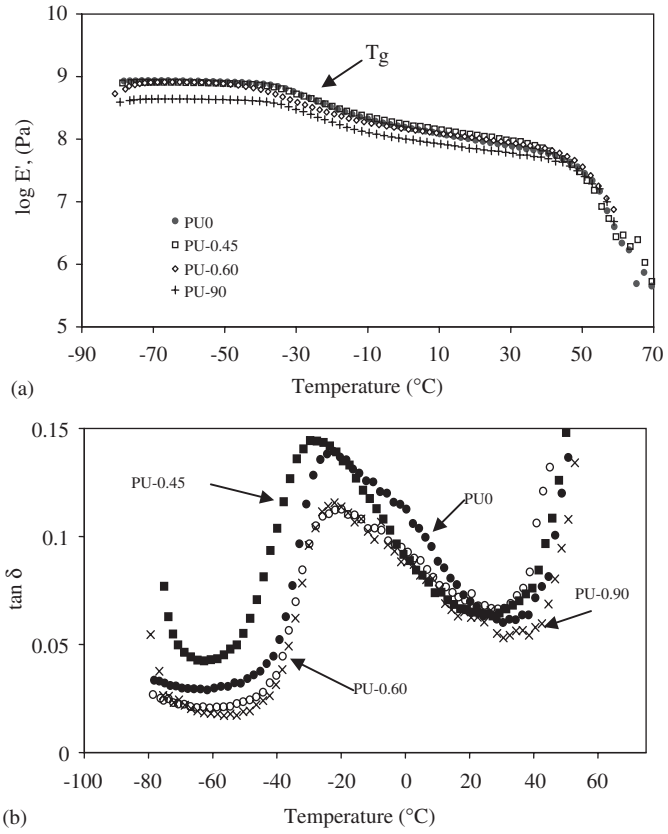

Fig. 12. (a) Variation of the elastic module (E') of the nanosilica–polyurethane mixtures as a function of the temperature. (b) Variation of the loss tangent ($\tan\delta$) of the nanosilica–polyurethane mixtures as a function of temperature. DMTA experiments.

nanosilica (PU-0.45 is given as a typical example in Fig. 11b) and the material depicts an elastic behaviour over the whole temperature range, indicating the creation of interactions between the polyurethane and the silanol groups of the nanosilica.

The viscoelastic properties of the polyurethanes were characterized by using DMTA. Fig. 12a shows the variation of the storage module (E') of the nanosilica–polyurethane mixtures as a function of temperature. These curves show three different zones: (i) At low temperature up to about $-40\,^{\circ}C$ there is the zone of the glassy region, in which the storage modulus is high and it does not vary as temperature increases; the storage modulus is slightly lower for PU-0.90; (ii) the glass transition region (identified by an inflexion point, Fig. 12a); and (iii) the rubber plateau followed by a drop of the storage modulus due to the melting of the soft segments. The different nanosilica–polyurethane mixtures show relatively similar curves. To better show the differences between the nanosilica–polyurethane mixtures, the variation of the loss tangent ($\tan\delta$) as a function of the temperature is given in Fig. 12b. PU0 and PU-0.45 have the largest area under the $\tan\delta$ curves indicating a lower degree of interaction between the HDK V15 nanosilica and the polyurethane. On the other hand, the glass transition is more clearly evidenced at the maximum of the $\tan\delta$ curves. The T_g values of the polyurethanes are located between -20 and $-24\,^{\circ}C$, being independent of the addition of nanosilica and the specific surface area and silanol content of the nanosilica.

The tensile strength and elongation at break of the nanosilica–polyurethane mixtures were measured by stress–strain tests. Figs. 13a and b show the variation of the tensile strength and elongation at break as a function of the silanol content on the nanosilica. The addition of nanosilica increases both the tensile strength and elongation at break of the polyurethane. In general, there is an improvement in tensile strength and elongation at break by increasing the silanol content. In fact, for tensile strength, up to $0.6\,mmol/g_{silica}$, and for elongation at break, up to $0.45\,mmol/g_{silica}$, have the largest effect, respectively. Therefore, the interactions between the silanol groups on the nanosilica and the polyurethane determine the mechanical properties of the mixtures.

Finally, the adhesive strength values of PVC/nanosilica–polyurethane adhesive joints as a function of time after

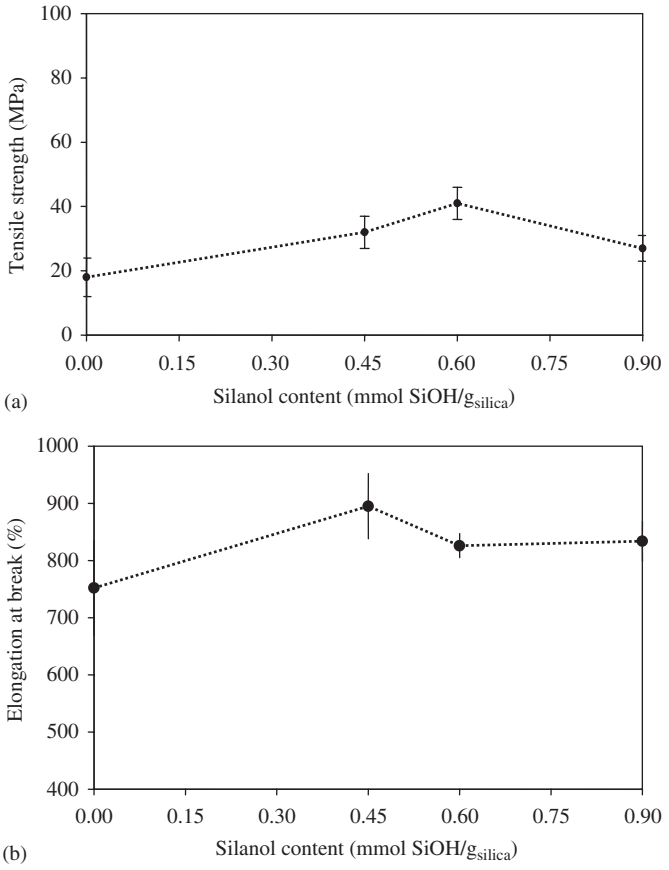

Fig. 13. (a) Tensile strength and (b) elongation at break of the nanosilica–polyurethane mixtures as a function of the silanol content on the nanosilicas.

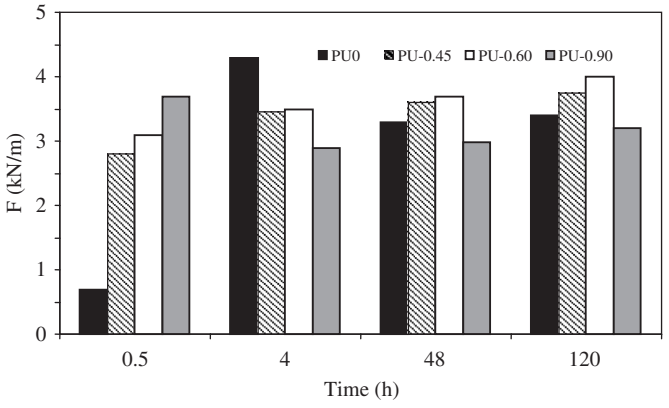

Fig. 14. *T*-peel strength values of PVC/nanosilica–polyurethane adhesive joints as a function of the time after joint formation. Loci of failure were assessed by visual inspection : Always a cohesive failure within the adherent was obtained, except for the joints peeled 0.5 h after joint formation.

bond formation are given in Fig. 14. The immediate adhesion (obtained 30 min after bond formation) is much higher in the joints produced with the polyurethane adhesives containing nanosilica, the higher the silanol content the higher the increase in the immediate peel strength. Because an interfacial failure between the PVC and the adhesive (assessed by visual inspection) was always obtained, the trend in immediate adhesion can be ascribed to the incidence of the rheological properties (Fig. 11) of the polyurethane–nanosilica mixture. The *T*-peel strength increases 4 h after joint formation because the crystallization of the polyurethanes is produced (Fig. 14). Small differences in peel strength values are obtained by increasing the time after joint formation up to 120 h, and the final adhesion is somewhat higher in the joints produced with the polyurethane adhesives containing nanosilicas. The results from these tests (4, 48 and 120 h) were invariably cohesive within the PVC (assessed by visual inspection). Therefore, the properties of the polyurethanes containing nanosilicas with different silanol content become relevant. Although a cohesive failure in the PVC was always obtained, it is interesting to note that, for the filled adhesives, a slight though progressive increase in joint strength was found with the passage of time with the ordering of the three systems (PU-0.45, PU-0.60 and PU-0.90) remaining unchanged with the PU-0.60 system the stronger and the PU-0.90 system the weaker. This is in agreement with the trends shown in the viscoelastic (Fig. 12) and mechanical properties (Fig. 13) of the filled adhesives. Therefore, the viscoelastic and mechanical properties of the filled adhesives determine their adhesion to PVC.

4. Conclusions

In this study it has been shown that a relationship between the degree of phase separation in the polyurethane and the specific surface area and silanol group content of the nanosilicas existed. The increase in the degree of phase segregation was due to the creation of interactions between the silanol groups on the nanosilicas and the polyurethane, favouring the creation of inter-urethane bonds which allowed the soft segment chains to move more freely. The creation of these interactions produced a decrease in the crystallization and melting enthalpies of the polyurethanes containing nanosilicas. On the other hand, the addition of nanosilicas increased the thermal stability of the polyurethanes, irrespective of the nanosilica specific surface area and silanol content.

The nanosilica–polyurethane mixtures showed a greater storage and loss moduli than the polyurethane alone due to the interactions produced between the nanosilica and the polyurethane, and the cross-over between the storage and loss moduli disappeared. On the other hand, the area under the maximum of the $\tan\delta$ curves of the polyurethanes decreased by adding nanosilica as a consequence of the interactions produced between them. The immediate peel strength values of the PVC/polyurethane adhesives joints increased in the joints produced with adhesives containing nanosilica, in a greater extent by increasing the specific surface area and silanol content of the nanosilica. Finally,

although a cohesive failure in the PVC was always obtained, a slight though progressive increase in joint strength was found with the passage of time (4, 48 and 120 h) with the ordering of the three systems (PU-0.45, PU-0.60 and PU-0.90) remaining unchanged with the PU-0.60 system the stronger and the PU-0.90 system the weaker. This is in agreement with the trends shown in the viscoelastic and mechanical properties of the filled adhesives

Acknowledgements

José Vega-Baudrit thanks the Santander Central Hispano Bank (Alicante, Spain) for granting his Ph.D. studies. The authors thank Wacker-Chemie (Burghausen, Germany) for providing the nanosilicas used in this study and Dr. A. Hartwig (Institut Fertgungstechnik Materialforschung—IFAM, Germany) for measuring the FTIR spectra of the nanosilicas. The authors also thank CONICIT-MICIT, Universidad Nacional of Costa Rica and POLIUNA for their support during this research.

References

[1] Oertel G. Polyurethane handbook. 2nd ed. New York: Hanser; 1993. p. 7 [chapter 2].
[2] Maciá-Agulló TG, Fernández-García JC, Pastor-Sempere N, Orgilés-Barceló AC, Martín-Martínez JM. J Adhes 1992;38:31.
[3] Jaúregui-Beloqui B, Fernández-García JC, Orgilés-Barceló AC, Mahiques-Bujanda MM, Martín-Martínez JM. J Adhes Sci Technol 1999;13:695.
[4] Jaúregui-Beloqui B, Fernández-García JC, Orgilés-Barceló AC, Mahiques-Bujanda MM, Martín-Martínez JM. Int J Adhes Adhes 1999;19:321.
[5] Torró-Palau A, Fernández-García JC, Orgilés-Barceló AC, Martín-Martínez JM. Int J Adhes Adhes 2001;21:1.
[6] Pérez-Limiñana MA, Torró-Palau AM, Orgilé-Barceló AC, Martín-Martínez JM. Macromol Symp 2001;169:191.
[7] Navarro-Bañón V, Vega-Baudrit J, Vázquez P, Martín-Martínez JM. Macromol Symp 2005;221:1.
[8] Tien Y, Wei K. Polymer 2001;42(7):3213.
[9] Nunes RCR, Fonseca JLC, Pereira MR. Polym Test 2000;19:93.
[10] Nunes RCR, Pereira RA, Fonseca JLC, Pereira MR. Polym Test 2001;20:707.
[11] Vega-Baudrit J, Navarro-Bañón V, Vázquez P, Martín-Martínez JM. Int J Adhes Adhes 2006;26:378.
[12] Vega-Baudrit J. PhD thesis, University of Alicante, June 2005.
[13] Brunauer S, Emmett PH, Teller E. J Am Chem Soc 1938;60:809.